ORGANOMETALLICS

Article

pubs.acs.org/Organometallics

A Three-Stage Mechanistic Model for Ammonia–Borane Dehydrogenation by Shvo's Catalyst

Zhiyao Lu, Brian L. Conley, and Travis J. Williams*

Loker Hydrocarbon Research Institute and Department of Chemistry, University of Southern California, Los Angeles, California 90089-1661, United States

Supporting Information

ABSTRACT: We propose a mechanistic model for three-stage dehydrogenation of ammonia–borane (AB) catalyzed by Shvo's cyclopentadienone-ligated ruthenium complex. We provide evidence for a plausible mechanism for catalyst deactivation and the transition from fast catalysis to slow catalysis and relate those findings to the invention of a second-generation catalyst that does not suffer from the same deactivation chemistry. The primary mechanism of catalyst deactivation is borazine-mediated hydroboration of the ruthenium species that is the active oxidant in the fast catalysis case. This transition is characterized by a change in the rate law for the reaction and changes in the apparent resting state of the catalyst. Also, in this slow catalysis situation, we see an additional intermediate in the sequence of boron, nitrogen species, aminodiborane. This occurs with concurrent generation of NH_3, which itself does not strongly affect the rate of AB dehydrogenation.

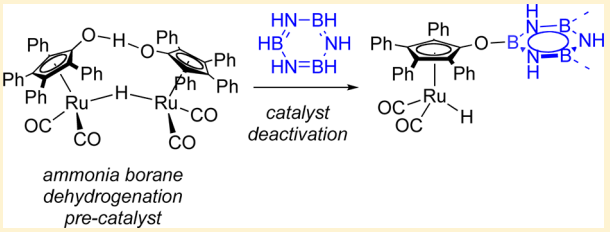

INTRODUCTION

Hydrogen is an attractive alternative transportation fuel that has appeal because it is carbon-free, is easily oxidized in fuel cells, and is potentially available from water electrolysis.[1] Although pressurized hydrogen gas currently has some use in vehicles, its practicality in cars is limited by fuel range, convenience, and safety concerns.[2] Particularly, hydrogen has low volumetric energy density (5.6 MJ/L at 700 bar) despite high mass energy density (120 MJ/kg for hydrogen).[3] Thus, a highly weight-efficient strategy to store hydrogen as condensed matter might enable its translation more broadly into transportation applications and consumer products.

Ammonia–borane (AB) is a promising material from which to build a practical hydrogen storage system, because it has high hydrogen density (19.6 wt %, ca. 9.9 MJ/L, 12.6 MJ/kg) and it can release hydrogen under mild conditions (thermolysis, hydrolysis, and catalysis; Figure 1).[4] Transition-metal-catalyzed dehydrogenation of ammonia–borane, particularly, is an area of active research interest because it may enable a more efficient fuel cycle than the well-known catalytic hydrolysis reaction that forms ammonia, which is poisonous to fuel cells, and strong B–O bonds, which are energetically costly to rereduce.[5] Several active transition-metal-based catalysts have been reported for AB dehydrogenation reactions, in either heterogeneous or homogeneous systems; these involve rhodium,[6] iridium,[7] ruthenium,[8−10] nickel,[11] palladium,[12] and iron catalysts,[13] among others[14] (Figure 2).

Our laboratory's studies on catalytic AB dehydrogenation have been focused on the reactivity of Shvo's catalyst (**12**, Scheme 1)[15] and its relatives. By analogy to the established mechanism for alcohol oxidation with **12**, we presumed that the

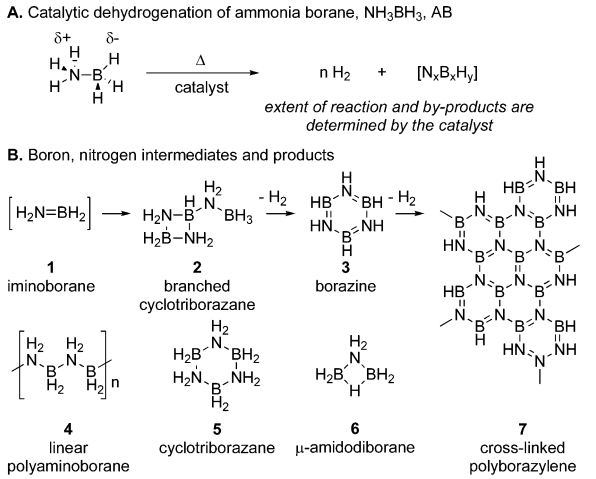

Figure 1. Ammonia–borane dehydrogenation reactions and possible products.

coordinative saturation of the reduced form of the Shvo system would preclude coordination of aminoborane, NH_2BH_2, to the catalyst, and thus disfavor the formation of insoluble oligomers, $[NH_2BH_2]_n$, which limits the hydrogen production of some catalysts[7,8] for ammonia–borane dehydrogenation to 1 equiv.[16] Although this proposal seems to hold true,[9] the catalyst begins to deactivate after ca. 25% conversion in the first pass, which renders this system irrelevant to practical implementation.

Received: June 19, 2012
Published: August 30, 2012

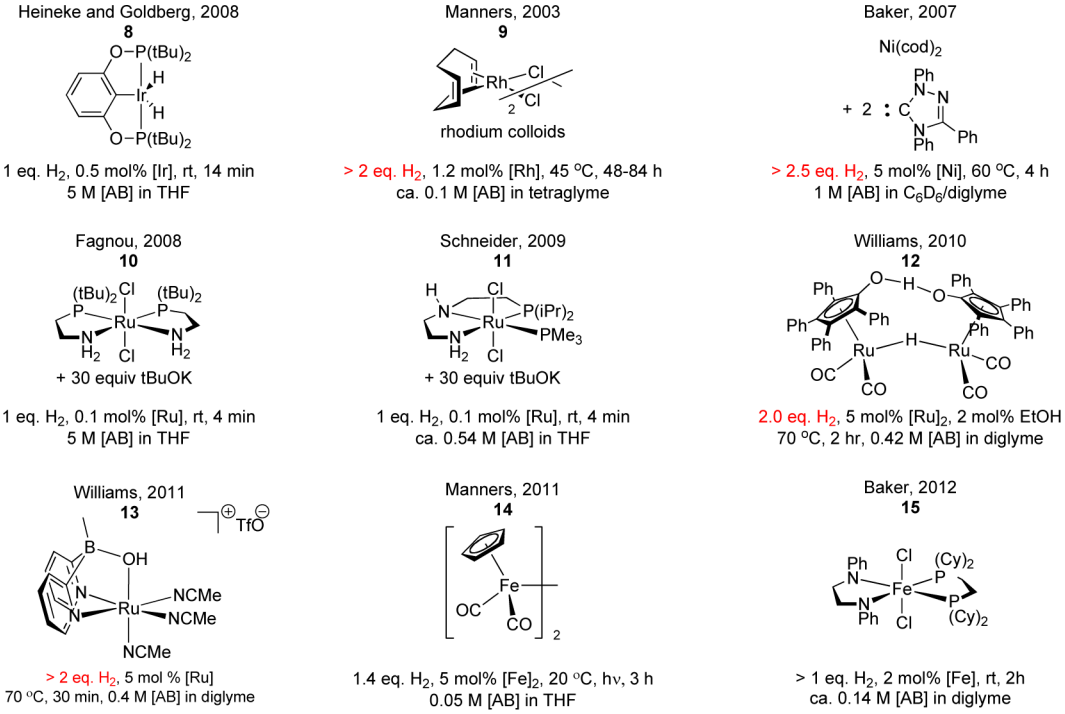

Figure 2. Transition-metal catalysts for AB dehydrogenation.

Scheme 1. Dehydrogenation of AB with Shvo's Catalyst, 12

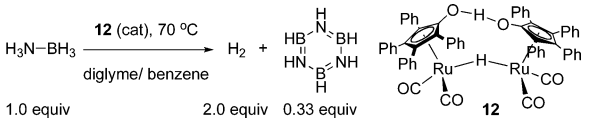

This text examines the molecular events that deactivate the Shvo catalyst in ammonia–borane dehydrogenation. These include hydroboration of the active, oxidizing form of the catalyst by borazine, which involves the borylation of the catalyst's ligand oxygen atom so that the turnover-limiting H–H bond-forming step is no longer accessible. Ultimately, we addressed this problem by designing a second-generation system, **13**,[17] that does not rely on an oxygen center as a proton acceptor in the same way as the Shvo catalyst. This second-generation system then enables access to high weight efficiency dehydrogenation of ammonia–borane.[10]

RESULTS AND DISCUSSION

The kinetic profile of AB dehydrogenation with **12** shows complicated behavior that we deconvoluted into a sequence of three limiting cases (Figure 3).[9] In our prior work we described cases 1 and 2 in detail:[9] catalyst initiation and fast catalysis, respectively. The former is the case of low conversion and zero [borazine] with ruthenium beginning in its dimeric form. This can be easily studied in isolation, because these are the conditions at the beginning of the reaction and because initiation occurs quickly at 55 °C, where the catalysis is slow. The second case is the one in which AB conversion and [borazine] are low and the ruthenium in the system is no longer in the form of its dimeric precursor. This case can easily

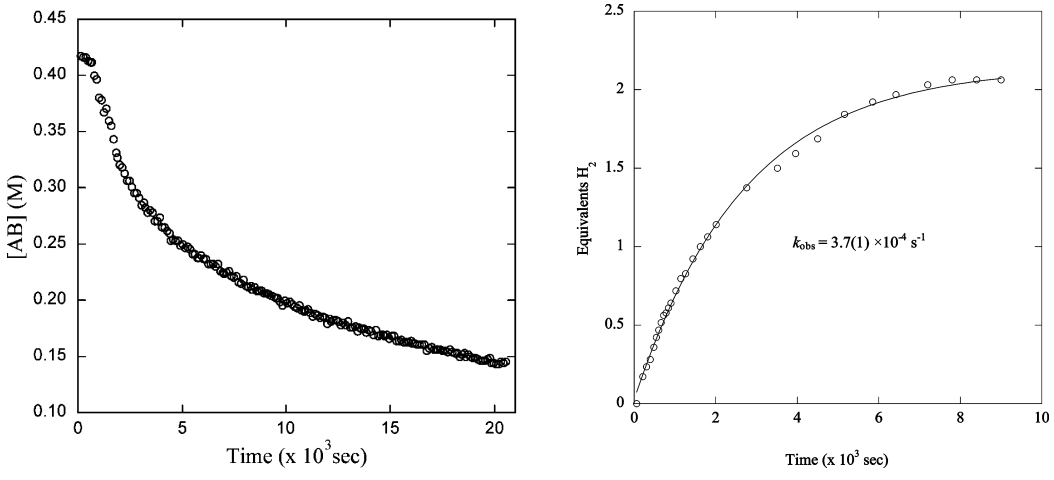

Figure 3. (left) ^{11}B NMR data showing consumption of AB in the presence of 2.5 mol % **12** in a sealed J. Young NMR tube. (right) Eudiometer data showing production of hydrogen gas in the presence of 5.0 mol % **12** and 2.0 mol % ethanol in 2/1 diglyme/benzene-d_6 at 70 °C.

dx.doi.org/10.1021/om300562d | Organometallics 2012, 31, 6705–6714

be studied in isolation by either (1) allowing the reaction to incubate at room temperature until it is initiated, i.e. **12**'s characteristic μ-H peak ($\delta(^1H)$ −17.7 ppm) is consumed, or (2) delivering the ruthenium as dimer **18** (vide infra, Scheme 2). The third case, slow catalysis, occurs under the condition that [borazine] ≈ [Ru atoms]. In this case the rate of dehydrogenation catalysis drops precipitously and the catalyst "dies". This case can be generated in isolation by adding a catalytic portion (1 equiv versus [Ru_{atom}]) of borazine to the reaction mixture at the outset of dehydrogenation.[9]

Figure 3 shows (left) AB consumption and (right) H_2 generation as functions of time for trials of dehydrogenation that cycle through all three of its mechanistic cases.[9] This is particularly evident from AB consumption: AB is consumed slowly as the catalyst initiates (case 1) and then it is consumed more quickly once dimer **12** is cleaved. Ultimately, [borazine] increases and the catalysis slows down.

Understanding the mechanism of dehydrogenation in the high [borazine] case and the catalyst deactivation process is particularly important for the following reasons. (1) The kinetic profile of the AB consumption in the high [borazine] case is that observed when the catalyst is reused, and reusability is essential for practical applications. (2) Borazine is an unavoidable intermediate in AB dehydrogenation if ≥2 mol equiv of hydrogen is released, yet the coordination chemistry of borazine is not well studied in the context of catalytic AB dehydrogenation systems.[3] Understanding the mechanism of this deactivation is important for the design of more efficient catalytic systems and, ultimately, a broadly useful solution to reversible hydrogen storage on ammonia−borane.

I. Catalyst Initiation (Case 1). A short period in the beginning of the reaction (ca. 2% conversion) is an initiation period in which AB consumption is slow. This situation can be studied in isolation by monitoring the reaction at a temperature well below that needed for fast catalysis, 70 °C. Thus, upon heating to 55 °C, the bridging hydride in **12** ($\delta(^1H)$ −17.7 ppm) is replaced by the hydride of monomeric species **16** ($\delta(^1H)$ −10.0 ppm) at a rate of $7.96(21) \times 10^{-4}$ s^{-1}.[9] This indicates that Shvo's catalyst, **12**, dissociates to its reduced monomer **16** and (presumably) oxidized monomer **17** (Scheme 2A). ^1H NMR integrations show that 2 equiv of **16** is formed with consumption of **12**; thus, the reduction of **17** is rapid relative to dissociation of **12**.

The finding of rapid reduction of **17** by ammonia−borane is supported by the relatively rapid rate of reduction of **18**, a stable dimer of **17**, under analogous conditions (Scheme 2B).

Scheme 2. Catalyst Initiation[a]

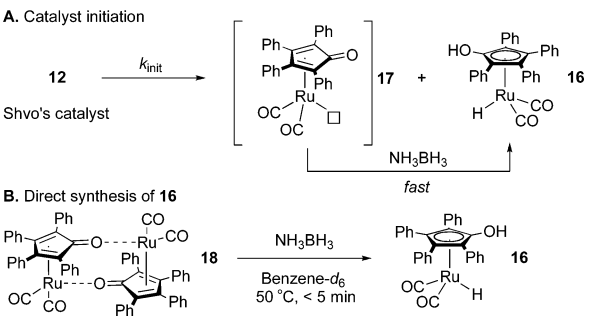

[a]A: scheme for catalyst initiation. B: rapid formation of **16** from **18**. [AB] is 0.42 M in benzene-d_6 solution, and $[Ru]_2$ is 5 mol % to AB.

In this experiment we see that conversion of **18** to **16** reaches completion within 5 min at 50 °C (see the Supporting Information). This corresponds to a rate constant of $>10^{-2}$ s^{-1} at 50 °C, which is faster than the rate of catalyst initiation (10^{-3} s^{-1} at 55 °C). Thus, the dissociation of dimer **12** is rate-limiting in catalyst initiation. This result is in accordance with Shvo's considerable dissociation enthalpy: 28.8 kcal/mol in toluene in the absence of AB.[18b]

II. Fast Catalysis (Case 2). After the catalyst initiation, the kinetic profile of AB consumption displays fast, linear kinetics through ca. 20−30% conversion. In these conditions, the reaction has a zero-order dependence on [AB] and first-order dependence on the catalyst's [Ru], as determined by the respective zero and unity slopes of plots of ln k_{obs} versus ln [AB] and ln [Ru].[9] Throughout this case, ^1H NMR shows a persistent monomeric ruthenium hydride at $\delta(^1H)$ −10 ppm, which is plausibly the resting state of the catalyst. This is consistent with H−H bond formation as the turnover-limiting step in fast catalysis. This assignment is consistent with the observed kinetic dependencies of $[AB]^0$ and $[Ru]^1$. We further observe first-order dependence on [EtOH], which is consistent with the transition state model established by Casey for stoichiometric hydrogen loss from **16**.[18] Thus, we adopt Casey and Cui's geometry for ethanol-mediated H−H bond formation from **16** as the turnover-limiting transition state of this catalysis (Scheme 3). In sum, the observed rate law in this case of the reaction is $-d[AB]/dt = k_{obs}[Ru][EtOH]$.

Scheme 3. Proposed Mechanism of Fast Catalysis (Case 2)

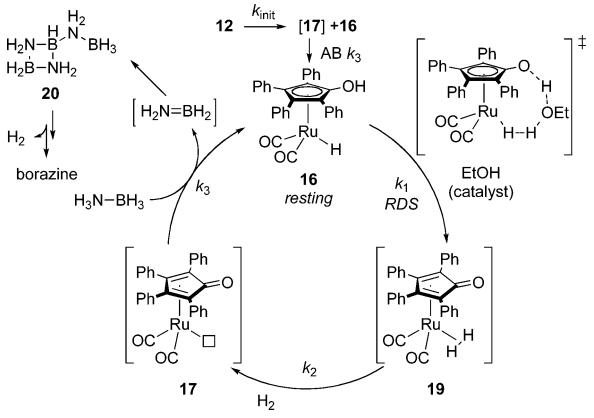

III. Slow Catalysis (Case 3). *Kinetics of Ammonia−Borane Dehydrogenation in the Slow Catalysis Case.* Onset of the slow catalysis conditions, i.e. catalyst deactivation, is characterized by the appearance of curvature in the time course plot of [AB], and it becomes more likely as [borazine] rises. The conditions of slow catalysis cause the emergence of multiple κ^1-Ru−H hydride peaks (from $\delta(^1H)$ −9 to −10 ppm), which occurs simultaneously with exponential decay behavior in [AB]. We believe that these correspond, respectively, to (a) new resting state(s) of the catalyst and ammonia−borane's role in a new turnover-limiting step. Understanding this mechanism is essential to our studies on catalyst reuse and, we infer, spent fuel regeneration.

An essential feature of the high [borazine] case of the reaction is that the catalyst is reusable within the limits of its kinetics. Thus, if a completed reaction mixture is treated with a new aliquot of ammonia−borane, dehydrogenation will recommence upon heating, and the reaction's kinetic profile

dx.doi.org/10.1021/om300562d | *Organometallics* 2012, 31, 6705−6714

will follow slow catalysis behavior wherein the rate of hydrogen production is too slow to be useful.[9] It is easy to believe that, at the conclusion of the reaction, the concentration of [**17**] is very small, so that dimer **12** is not re-formed, and it is unnecessary to repeat catalyst initiation (case 1) in catalyst reuse experiments. However, the absence of fast catalysis must result from a practically irreversible deactivation of the catalyst during the transition from fast catalysis to slow catalysis in the first run.

The exponential decay shape of the kinetic profile of AB consumption suggests that the reaction is now first order in [AB] in the slow catalysis regime (Table 1, left), as verified by a plot of ln k_{obs} versus ln [AB] with a slope of 1.03(4) as recorded in the case of high [borazine]. This draws a significant contrast to fast catalysis, where such a plot was of zero slope, and indicates that, unlike fast catalysis, once the catalyst deactivates, the turnover-limiting step for further turnover involves conversion of the resting species by 1 equiv of ammonia–borane.

Table 1. Ammonia–Borane Consumption as a Function of [AB] and [Ru] in Slow Catalysis[a]

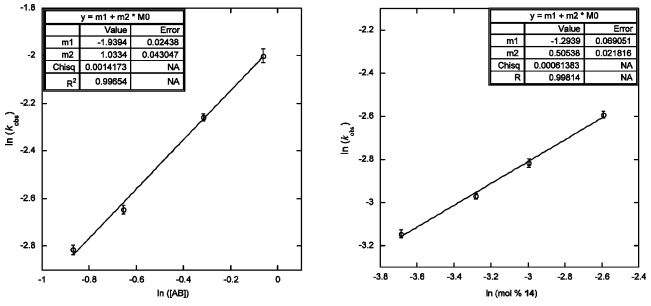

AB (M)	rate (k_{obs}) (s^{-1})[b]	amount of **12** (mol %)	rate (k_{obs}) (s^{-1})[c]
0.42	$5.99(12) \times 10^{-5}$	2.5	$4.31(7) \times 10^{-5}$
0.52	$7.09(19) \times 10^{-5}$	3.75	$5.13(6) \times 10^{-5}$
0.73	$1.05(2) \times 10^{-4}$	5.0	$5.99(12) \times 10^{-5}$
0.94	$1.35(4) \times 10^{-4}$	7.5	$7.49(12) \times 10^{-5}$

[a]Data calculated from ^{11}B NMR monitored kinetic studies at 70 °C. [b]$[Ru_{atom}]_0$ = 42.0 mM. [c]$[AB]_0$ = 0.42 M.

Isotope Effects. Kinetic isotope effects were determined for dehydrogenation of selectively deuterium-labeled ammonia–borane isotopologues[21] ND_3BH_3, NH_3BD_3, and ND_3BD_3 in high [borazine] conditions. Comparison of measured rate constants for parallel runs at 70 °C gave kinetic isotope effects of k_{NHBH}/k_{NDBH} = 1.46(3), k_{NHBH}/k_{NHBD} = 1.07(5), and k_{NHBH}/k_{NDBD} = 2.30(4) (see the Supporting Information). The KIE in NH is suggestive of a catalyst reactivation involving participation of the NH in its turnover-limiting step. This might be akin to a protonation of the resting state of the catalyst by an acidic NH proton. These data present a conundrum, however, which is that the product of the two single-label KIEs should equal the double-label KIE; in this case we have 1.46(3) × 1.07(5) = 1.56(6), which is well below the observed value of 2.30(4). Along these lines, Casey's group has reported H/D exchange of the Ru–H group in Shvo's catalyst with D_2 (or vice versa) of **16-Tol** in THF without substituting the corresponding ligand O–H.[18] Similarly, in two parallel runs of ND_3BH_3 dehydrogenation, similar portions of HD and H_2 were formed. The presence of H_2 (and by symmetry D_2) implies the availability of a mechanism for proton/hydride exchange under our catalytic conditions. On the basis of our observations and their result, we conducted an experiment of ND_3BD_3 dehydrogenation with 1 atm of H_2 gas applied to the solution. HD was formed during this reaction (Scheme 4A),

Scheme 4. H/D Exchange Experiments

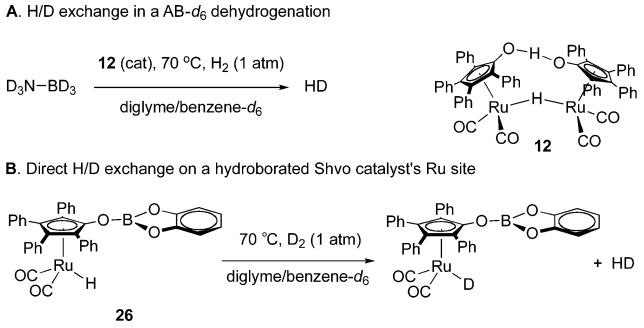

which necessitates an H/D crossover mechanism involving the final product, H_2. We believe that the mechanism of this is the same as Casey's H/D exchange mechanism, except we suggest that this mechanism is available to the resting state(s) of our catalyst. To test this latter hypothesis, we treated borylated ruthenium complex **26** with 1 atm of D_2 under conditions analogous to our catalytic reactions. We observed the formation of HD at room temperature in 5 min and complete deuteration in the hydride position of **26** within 1 h at 60 °C (Scheme 4B). This shows us that there is a mechanism for H/D exchange of the ruthenium hydride in an *O*-borylated homologue of the Shvo system. This result provides an explanation for the small experimental k_{NHBH}/k_{NHBD} value and the mismatch between our observed k_{NHBH}/k_{NDBD} and the value predicted by the separate values for proton and hydride: because there is a facile mechanism for H/D exchange, an isotopic kinetic resolution is possible.

Mechanistic Proposal. We propose, on the basis of NMR observations, that fast catalysis ends (i.e., catalyst deactivaiton occurs) because borazine undergoes a hydroboration with ruthenium intermediate **17** to give the deactivated complex **21**, which further converts to other derivatives (Scheme 5).[9] Reactions analogous to the addition of **3** to **17** are known from the Casey[18a] and Clark[22] laboratories (Scheme 6). Casey has shown hydrosilylation of the Shvo scaffold by triethylsilane. This adduct, **24-Tol**, has a $\delta(^1H)$ value of −9.20 ppm in benzene-d_6. Similarly, Clark has shown hydroboration of the Shvo complex with pinacol–and catechol–boranes in high yield at mild temperature. These adducts have $\delta(^1H)$ values of −9.33 and −9.26 ppm in benzene-d_6, respectively.

We propose that this hydroborated species can dimerize to form a O–B–O and Ru–H–Ru bridged dimer (**31**, Scheme 5) akin to the parent Shvo complex and Clark's [(μ-(cat)B-($C_4Ar_4O)_2$)$Ru_2(CO)_4(\mu$-H)] dimer, which accounts for the

dx.doi.org/10.1021/om300562d | *Organometallics* 2012, 31, 6705–6714

Scheme 5. Proposed Borazine-Mediated Hydroboration

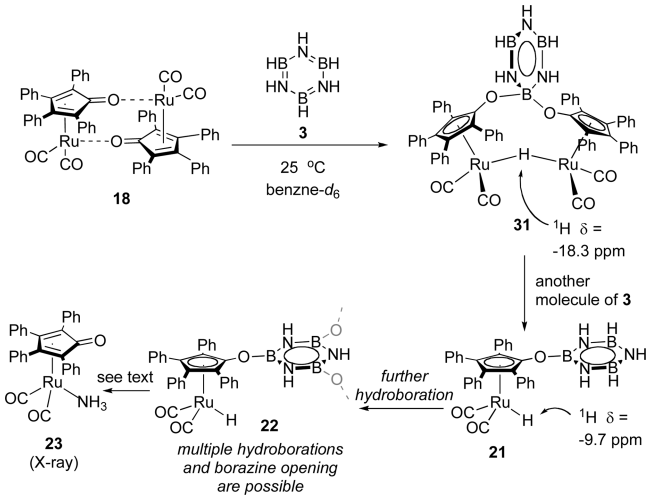

Scheme 6. Hydroboration and Hydrosilylation of Tol-18

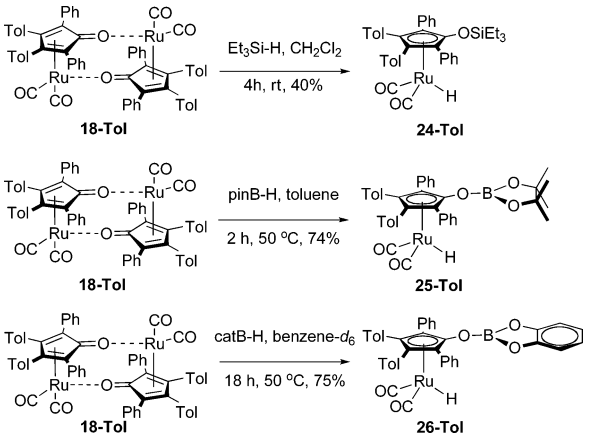

observed half-order kinetic dependence on [Ru]. These species can re-enter the catalytic cycle if the B–O bond affixing borazine to the catalyst is cleaved in the presence of ammonia–borane, which accounts for its first-order kinetic dependence. We do not know the mechanism of ammonia–borane's involvement in this step.

Catalyst Deactivation. We conducted a series of experiments directly to interrogate our proposal for the mechanism of slow catalysis, yet we observe that the proposed complex **21** is not stable to isolation. Borazine was added to dimer **18** at room temperature, and a bridging hydride peak formed at the beginning of the reaction ($\delta(^1H)$ −18.3) was then consumed in 2 min (Scheme 5). This was replaced by a set of 13 hydride peaks from $\delta(^1H)$ −9.3 to −10.0 ppm, which correspond to κ^1-Ru–H groups such as **22**. We suspect that these signals correspond to multiple hydroboration events on a single borazine or ring-opened borazine derivatives.

We can create slow catalysis case conditions at the beginning of a dehydrogenation reaction very simply by adding 1 mol equiv of borazine relative to [Ru_{atom}] to the reaction mixture prior to heating. Under these conditions the kinetic profile of the reaction does not show any properties of initiation or fast catalysis but proceeds directly to the rate and rate law of slow catalysis.[9] This is strong evidence indicating that borazine is the agent that causes catalyst deactivation and aptly accounts for the instant slow catalysis situation that is observed in catalyst reuse experiments. Because of their self-reactive nature, we are unable to isolate these complexes directly, but when a mixture of these materials is collected and excess borazine is quantitatively removed under reduced pressure, the resulting material can be isolated through aqueous workup. This treatment cleaves any borazine rings remaining in the borazine–catalyst complex(es) and affords a ruthenium-containing adduct, ammonia complex **23**,[23] which can be isolated in 42% yield. This observation gives strong evidence that the deactivated catalyst, the one present in the slow catalysis case, is covalently bound to a borazine moiety, because NH_3 could not have been delivered in any other plausible way.

An Analogue of the Deactivated Catalyst. Because our efforts to isolate and characterize our proposed deactivated catalyst were frustrated by its reactivity, we set about to devise a borazine analogue with which we could hydroborate **18** and generate a stable surrogate of the catalyst of the slow catalysis case. The premise of this design was our hypothesis that multiple equivalents of **17** are hydroborated by 1 equiv of borazine to yield multiple κ^1-Ru–H signals in the ^{1}H NMR spectrum. Along these lines, we prepared diazaborane **29** and treated it with dimer **18**. The result was near-quantitative formation of **12** under rigorously anhydrous conditions (Scheme 6). We infer from this result that proposed dimer **27**, if formed, apparently loses a borabenzoimidazole rapidly to regenerate **12**. In contrast, hydroboration of **18** with catecholborane to form **26** is facile and gives an oxygen-substituted analogue of our proposed deactivated catalyst that is free of N–H groups.

In situ preparation of **26** in a benzene/diglyme solution affords an opportunity to compare the rate and kinetic profile of **26**-catalyzed ammonia–borane dehydrogenation with those of the slow catalysis case (Scheme 7). The kinetic profiles each

Scheme 7. Synthesis of a Mechanistic Analogue for the Proposed Deactivated Catalyst Complex

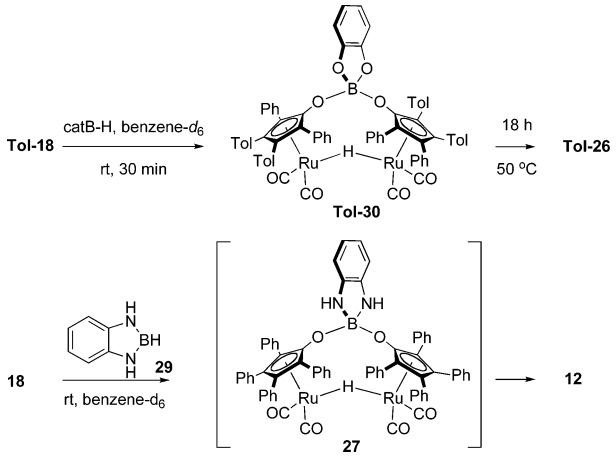

appear first order in AB, but the rate for dehydrogenation with catalyst precursor **26** is faster than slow catalysis by a factor of ca. 3-fold. This faster rate could be a result of a more labile O–B bond between the catalyst's hydroxycyclopentadiene and the corresponding boranes. A plot of ln k_{obs} versus ln [Ru] gave a slope of 0.51(3) (Table 2), which is in agreement with the measured [Ru] dependence for slow catalysis. These data show us that the dimerization behavior that we see in the slow catalysis case is effectively recreated in borylated analogue **26**. Taken together, these data provide good anecdotal evidence

dx.doi.org/10.1021/om300562d | *Organometallics* 2012, 31, 6705–6714

Table 2. Ammonia–Borane Dehydrogenation Catalyzed by Borylated Complex 26

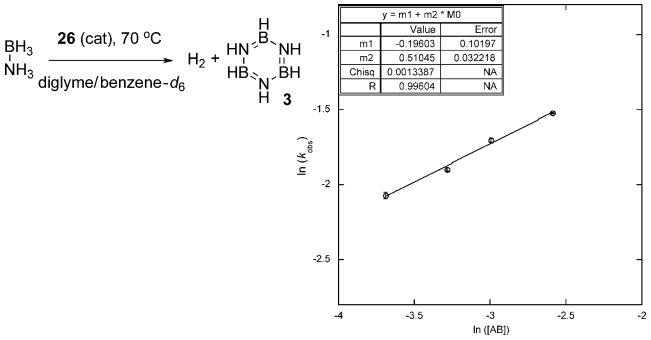

amount of **26** (mol %)	rate (s^{-1})
5.0	$1.26(3) \times 10^{-4}$
7.5	$1.50(2) \times 10^{-4}$
10	$1.82(2) \times 10^{-4}$
15	$2.18(2) \times 10^{-4}$

that the deactivated catalyst is an *O*-borylated form of the precatalyst.

Other Reaction Products and Intermediates in the Slow Catalysis Case. Ammonia–borane dehydrogenation catalyzed by **12** generates multiple B, N intermediates throughout the reaction. In fast catalysis the intermediates detected by ^{11}B NMR are the same as those observed for other catalysts that are known to liberate multiple equivalents of hydrogen from ammonia–borane:[9−11] AB → branched cyclotriborazane (**2**) → borazine (**3**) (Figure 1A). In the slow catalysis case, however, a new species appears, aminodiborane **6** (Scheme 8). This

Scheme 8. Formation of 6

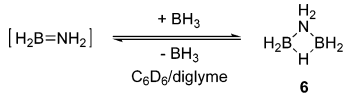

species should be dehydrogenated to borazine, and in fact, in reactions in which this species is an intermediate, borazine remains the only product upon completion of the reaction. We believe that **6** is an adduct formed from BH_3, dissociated from ammonia–borane, and NH_2BH_2, generated transiently after the first dehydrogenation of ammonia–borane.[16,24] We propose that formation of **6** is reversible, and this is only a mechanistic cul de sac, rather than an in-line intermediate in the dehydrogenation sequence. To test this hypothesis, we added (a) 0.5 equiv of 1 M BH_3·THF and (b) a comparable volume of THF to two otherwise identical runs of ammonia–borane dehydrogenation with **12** (Table 3). A strong signal for **6** was observed by ^{11}B NMR in tube a in the beginning of the reaction, much earlier than the first emergence of **6**'s peak in the THF control experiment (tube b). Both reactions proceeded through fast catalysis at about the same rate (Figure 3). Furthermore, the rates of AB consumption in slow catalysis case are similar, ca. 25% difference, which shows that although there is a large excess of **6** in tube a in comparison to the amount in tube b, this has a disproportionately small effect on the rate of AB consumption. We therefore know that **6** goes on to dehydrogenate to borazine and does not significantly interfere with the rates of the steps in slow catalysis as it forms and disappears. It further appears that BH_3 does not

Table 3. Rate of Slow Catalysis in the Presence and Absence of BH_3[a]

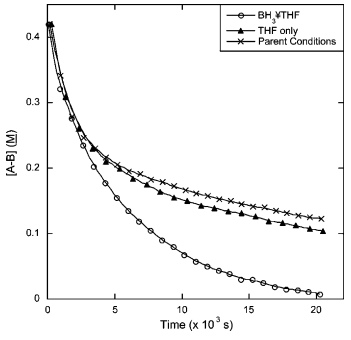

conditions	slow catalysis k_{obs} (s^{-1})
BH_3·THF	$1.57(7) \times 10^{-4}$
THF only	$7.0(13) \times 10^{-5}$
parent conditions[b]	$6.3(6) \times 10^{-5}$

[a]Data calculated from ^{11}B NMR kinetic studies at 70 °C. Smoothed curves are empirical fits; k_{obs} values shown are for slow catalysis, not the entire curve. See the Supporting Information. [b]A parallel run under parent conditions has k_{obs} in statistical agreement with others reported herein.

hydroborate and deactivate the catalyst in the same way as borazine or catecholborane.

If free BH_3 from the dissociation of ammonia–borane is impacting the course of the reaction in the slow catalysis case, then free NH_3 must also be present, and NH_3 is known to modulate the reactivity of the Shvo system.[23] Thus, we propose a second mechanism of catalyst deactivation, which is reversible formation of **23** by NH_3 ligation to the catalyst.

To interrogate directly the reactivity of ammonia adduct **23**, we prepared it independently through the addition of ammonia gas to **18** (Scheme 9). Analogous to the case for **12**, the ^{11}B

Scheme 9. Synthesis of Ammonia Adduct 23

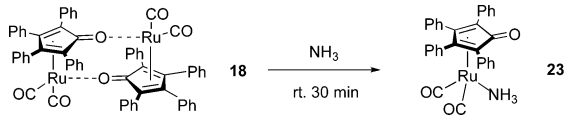

NMR kinetic profile of AB dehydrogenation with **23** appears to have two distinct kinetic cases, one linear case, with a reaction rate of 5.12×10^{-5} M s^{-1}, and one exponential decay case, with a rate constant of 4.22×10^{-4} s^{-1} (Table 4). This is similar to the second and third cases (fast and slow catalysis) of dehydrogenation with **12**, but since **23** is monomeric, it stands to reason that there should not be an initiation delay analogous to that observed in reactions featuring **12**. We account for this behavior by proposing that NH_3 reversibly can ligate **17** as previously documented[23] and thereby temporarily sequester it from its catalytic roles. Thus, NH_3 ligation provides a second mechanism for catalyst deactivation, although this one appears to be less deleterious than hydroboration of **17**.

Homogeneous versus Heterogeneous Catalysis. We propose that this reaction is homogeneous throughout its duration on the basis on four observations. First, the reactor maintains its homogeneous appearance through the duration of the reactions. No metallic residue is observed. Second, the rate of catalysis is not impacted by the addition of Hg(0). In contrast, a mercury drop does inhibit the catalytic hydro-

dx.doi.org/10.1021/om300562d | *Organometallics* 2012, 31, 6705–6714

Table 4. [AB] Dehydrogenation with 12 and 23[a]

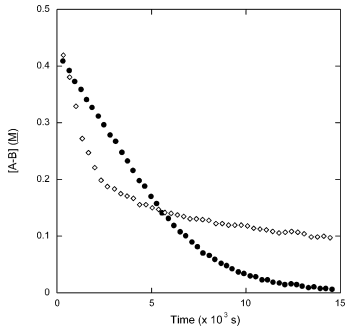

fast catalysis		slow catalysis	
cat.	rate ($M\ s^{-1}$)	cat.	k_{obs} (s^{-1})
12	$1.47(9) \times 10^{-4}$	**12**	$3.06(39) \times 10^{-4}$
23	$5.12(3) \times 10^{-5}$	**23**	$4.23(33) \times 10^{-4}$

[a]Data calculated from ^{11}B NMR kinetic studies. A 0.25 mol portion of AB and 0.035 mol of [Ru_{atom}] were added to 0.6 mL to diglyme/benzene-d_6. Both reactions were run at 70 °C. Black circles and diamonds are kinetic profiles of reactions catalyzed by **23** and **12**, respectively.

genation of benzene based on the $[Ru_3(\mu_2\text{-}H)_3(\eta^6\text{-}C_6H_6)(\eta^6\text{-}C_6Me_6)_2(\mu_3\text{-}O)]^+$ catalyst precursor, which is part of the evidence for heterogeneous reduction in that system.[25] This result is germane to the present discussion because it shows a documented system wherein the mercury drop experiment was effective with ruthenium. Still, the best evidence we have (third point) for homogeneous catalysis remains the foregoing kinetics data, in which the data remain pseudo first order in the slow catalysis case through >90% conversion (>3 half-lives). A fourth piece of evidence favoring homogeneous catalysis comes from a quantitative poisoning experiment wherein the reaction is run in the presence of a small portion of 1,10-phenanthroline.

Quantitative poisoning is an experiment in which less than 1 molar equiv (relative to the proposed monomeric catalyst) is introduced into the reaction, and one monitors the rate to see if it is affected proportionally to the concentration of the poison. If the drop in rate upon poisoning is disproportionally large, this can be evidence for heterogeneous catalysis, because <100% metal atoms (and often ≤50%)[26] are on the surface of a nanoparticle and thus ≤50% are available to be poisoned.

In this present case, two quantitative poisoning experiments were conducted wherein 0.1 and 0.5 equiv of 1,10-phenanthroline (phen) relative to [Ru_{atom}] were added to two otherwise standard ammonia–borane dehydrogenation runs with catalyst **12** (0.25 mol of AB, 70 °C, diglyme/benzene-d_6). Although these are not first-order reactions, generally we see that phen accelerates the reaction, apparently by prolonging the fast catalysis portion of the reaction (Figure 4). In contrast, 0.5 equiv of phen (relative to ruthenium atoms) completely quenches catalytic heterogeneous hydrogenation of benzene based on the $[Ru_3(\mu_2\text{-}H)_3(\eta^6\text{-}C_6H_6)(\eta^6\text{-}C_6Me_6)_2(\mu_3\text{-}O)]^+$ catalyst precursor.[25] Thus, we take our evidence to argue against the formation of a ruthenium nanoparticle. The origin of the acceleration behavior seems as if the phenanthroline "poison" is protecting the catalyst from borazine-mediated deactivation. This concept is further discussed in the Supporting Information.

A tetranuclear catalyst (e.g., Ru_4L_n) is unlikely but cannot be rigorously eliminated. Such a hypothesis is disfavored because

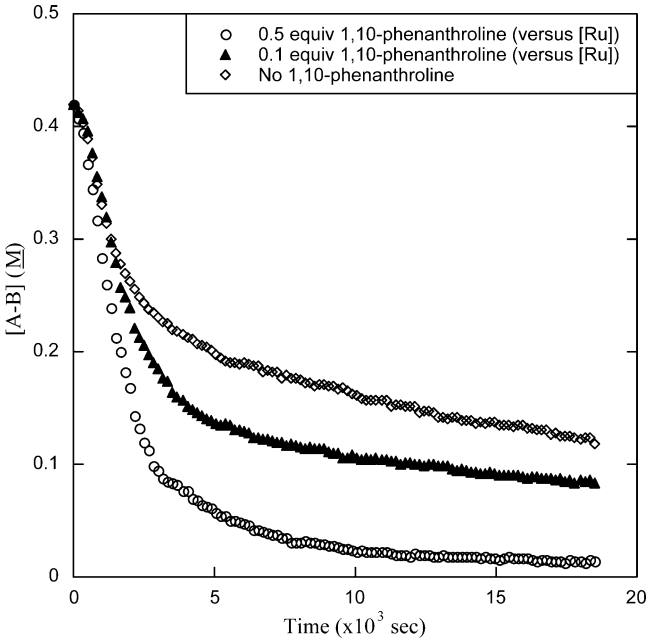

Figure 4. [AB] dehydrogenation with **12** in 1,10-phenanthroline. Data are calculated from ^{11}B NMR kinetic studies. A 0.25 mol amount of AB and 5 mol % of **12** were added to 0.6 mL of diglyme/benzene-d_6 at 70 °C.

an analogous $Rh_4Cp^*_{2.4}Cl_4H_c$ cluster has been shown to be the likely active catalyst in the hydrogen of benzene with $[Cp^*RhCl_2]_2$, and this Rh_4 cluster is deactivated by Hg(0).[27] Further, that Rh_4-based system is deactivated by 4 equiv of 1,10-phenanthroline (i.e., 1/1 phen/Rh_{atom}), while ours is not.

A Second-Generation Catalyst. To avoid the problem of catalyst *O*-borylation that is intrinsic to the deactivation of the Shvo catalyst, we devised the second-generation system highlighted in Scheme 10.[10,17] One design feature of this

Scheme 10. A Second-Generation Catalyst

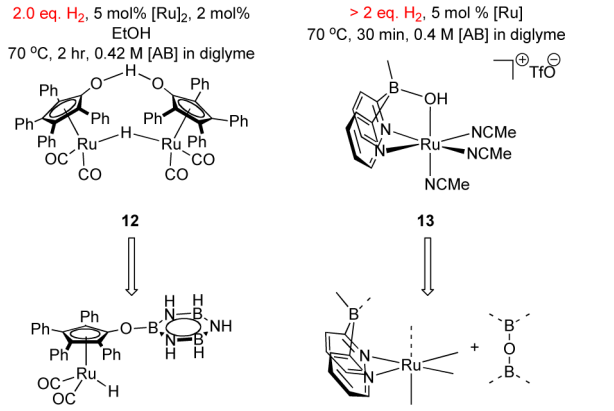

motif is that if the catalyst is borylated by analogy to **21**, the resulting borylated oxygen atom can be lost from the catalyst, so that the catalytic species is not deactivated. Although we do not know the mechanism of ammonia–borane dehydrogenation with **13**, we observe that it can liberate >2 equiv of H_2 from ammonia–borane, even on repeated uses and with exposure to the atmosphere, and it shows first-order consumption of ammonia–borane throughout conversion.

dx.doi.org/10.1021/om300562d | *Organometallics* 2012, 31, 6705–6714

CONCLUSION

In conclusion, we were able to propose a full picture of the catalyst deactivation mechanism (Scheme 11). A full scheme showing the origin of the slow catalysis case is illustrated in a diagram in the Supporting Information. The upper-right half of Scheme 11 is the fast catalysis mechanism, which is sketched in Scheme 3. We propose that catalyst deactivation is caused by the introduction of borazine, the product of selective dehydrogenation, into solution. When the rate of reduction of oxidized catalyst **17** by ammonia–borane becomes competitive with its hydroboration, AB consumption ceases to be linear. When hydroboration of **17** becomes fast relative to reduction of **17**, then **21** becomes a resting state of [Ru], and the catalysis "dies", as sketched in the lower-left half of the cycle in Scheme 11. In this phase of the reaction, conversion has first-order dependence on [AB], apparently because ammonia–borane is needed to convert borazine species **21** back into an active species.

Scheme 11. Mechanitic Proposal of Slow Catalysis

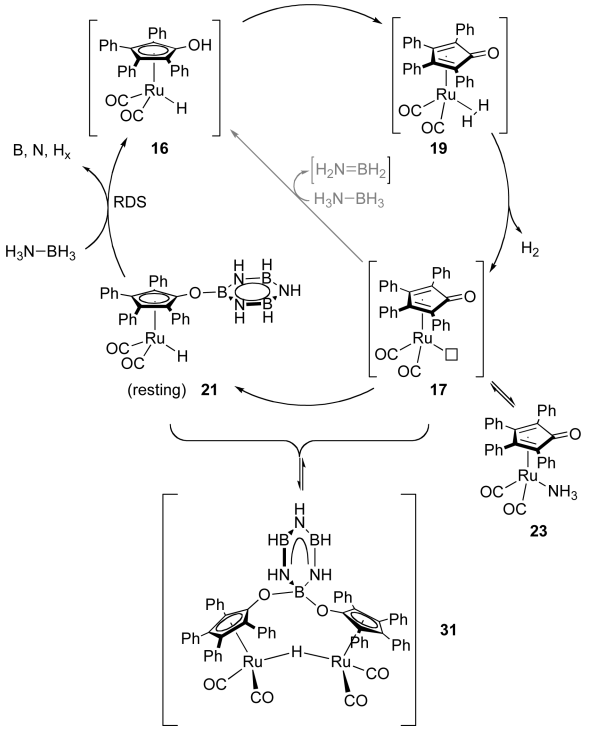

Reversible ammonia ligation of **17** is almost certainly happening throughout the reaction. We know, however, from the rates of (a) fast catalysis and (b) slow catalysis with ammonia complex **23** that **23** is a minor contributor to the total [Ru atoms] in fast catalysis because (i) the addition of 1 equiv of NH_3 relative to ruthenium slows fast catalysis and (ii) the rate of AB consumption is constant throughout the fast catalysis case. We also know that NH_3 ligation to ruthenium does not significantly alter the rate of slow catalysis.

In summary, the mechanism of AB dehydrogenation catalyzed by Shvo catalyst **12** was investigated. This reaction initiates with dissociation of the dimeric precatalyst **12** and then goes through a fast dehydrogenation reaction wherein the H–H bond formation is the turnover-limiting step. As the concentration of borazine increases, it adds to the reactive form of the catalyst to give ruthenium species, which are not as reactive as their mechanistic predecessor in ammonia–borane dehydrogenation. Presumably, these deactivated ruthenium species are reactivated by ammonia–borane itself and proceed to further ammonia–borane dehydrogenation. This observation gives us insight into the higher reactivity of our second-generation catalyst, **13**.

EXPERIMENTAL SECTION

I. General Procedures. All air- and water-sensitive procedures were carried out either in a Vacuum Atmospheres glovebox under nitrogen (0.5–10 ppm of O_2 for all manipulations) or using standard Schlenk techniques under nitrogen. Deuterated NMR solvents were purchased from Cambridge Isotopes Laboratories. Benzene-d_6 and diethylene glycol dimethyl ether (diglyme, J. T. Baker) were dried over sodium benzophenone ketyl and distilled prior to use. Shvo's catalyst was purchased from Strem Chemicals. Ammonia–borane (NH_3BH_3, AB) was purchased from Sigma Aldrich. Borazine was synthesized and purified by the method used by Wideman and Sneddon.[28] ^{1}H and ^{11}B NMR spectra were obtained on a Varian 600 spectrometer (600 MHz in ^{1}H, 192 MHz in ^{11}B) with chemical shifts reported in units of ppm. All ^{1}H chemical shifts are referenced to the residual ^{1}H solvent (relative to TMS). All ^{11}B chemical shifts are referenced to $BF_3{\cdot}OEt_2$ in diglyme in a coaxial external standard (0 ppm). NMR spectra were taken in 8 in. J. Young tubes (Wilmad) with Teflon valve plugs. The NMR tubes were shaken vigorously for several minutes with chlorotrimethylsilane and then dried in vacuo on a Schlenk line prior to use.

Caution! Extreme caution should be used when carrying out these reactions, as the release of hydrogen can lead to sudden pressurization of reaction vessels.

II. Mechanistic Studies Utilizing ^{11}B and ^{1}H NMR Spectroscopy. In a typical reaction, 7.7 mg of AB was combined with Shvo's catalyst (**12**, 13.6 mg, 5 mol %) in a J. Young NMR tube while in a glovebox under nitrogen. The AB and catalyst concentrations may be varied. Diglyme (0.4 mL) and benzene-d_6 (0.2 mL) were added to the tube, as was the BF_3 insert. The sample tube was immediately inserted into a preheated NMR (70 °C), and the kinetic monitoring commenced after quickly locking and shimming. Disappearance of AB in the solution was monitored by the relative integration of its characteristic peak in the ^{11}B spectrum (−22 ppm) and the $BF_3{\cdot}OEt_2$ standard. All spectra were processed using VNMRJ (version 2.3). The acquisition involved a 1.67 s pulse sequence in which 4096 complex points were recorded, followed by 1 s relaxation delay. To eliminate B–O peaks from the borosilicate NMR tube and probe, the ^{11}B FIDs were processed with back linear prediction, ca. 5–15 points.

A. Determination of Catalyst Order in Conversion of AB in Case 3 (Slow Catalysis). The rate values for the slow catalysis case were determined using ^{11}B NMR in sealed NMR tubes, as described above. Data treatments are shown in the Supporting Information. The amount of AB was 7.7 mg (0.25 mmol), and catalyst concentrations were varied (6.8, 10.2, 13.6, and 20.3 mg of **12**, (2.5, 3.75, 5.0, and 7.5 mol %)). The results were plotted as a ln/ln relationship to determine the order in catalyst (Table 1, right).

B. Determination of Order in AB in Case 3 (Slow Catalysis). The rate values for the slow catalysis case were again determined using ^{11}B NMR in sealed NMR tubes. Data treatments are shown in the Supporting Information. The amount of **12** was 13.6 mg (0.013 mmol), and AB concentrations were varied (7.7, 8.7, 13.5, and 17.4 mg AB (0.42, 0.53, 0.73, and 0.94 M)). The results were plotted as a ln/ln relationship to determine the order in ammonia-borane (Table 1, left).

C. Kinetic Isotope Effects in Case 3 (Slow Catalysis). To determine the kinetic isotope effects on the reaction rate, 8.5 mg of ND_3BH_3, 8.5 mg of NH_3BD_3, or 9.2 mg ND_3BD_3 (0.25 mmol) was added to a J. Young NMR tube. To each was added 13.6 mg of **12** (5 mol %), diglyme (0.4 mL), and benzene-d_6 (0.2 mL). Again, we analyzed [AB] vs time for the third case of the reaction conditions. Data treatments are shown in the Supporting Information. KIEs were determined from the quotient of protic AB k_{obs} ($5.99(12) \times 10^{-5}$ s^{-1}) divided by the deuterated AB k_{obs}. The HD signal found in the ^{1}H NMR resulted

dx.doi.org/10.1021/om300562d | *Organometallics* 2012, 31, 6705–6714

from H-D exchange and is also shown in Figure S5 (Supporting Information).

D. Kinetics for AB Dehydrogenation in the Presence of Added BH_3·THF. To examine the role of aminodiborane (**6**) in the mechanism of AB dehydrogenation, we manipulated its concentration by adding (tube A) 0.125 mL of 1 M BH_3·THF (0.125 mmol, 0.5 equiv to AB) or (tube B) 0.125 mL of THF to otherwise typical AB dehydrogenation reactions (7.7 mg (0.25 mmol) of AB, 13.6 mg (5 mol %) of **12**, 0.6 mL of 2/1 diglyme/benzene-d_6). ^{11}B NMR showed **6** (−26.7 ppm) in tube A at the beginning of the reaction (see the Supporting Information). The k_{obs} values for these runs were determined using ^{11}B NMR; data treatment is shown in the Supporting Information.

*E. Kinetics for AB Dehydrogenation by NH_3-Ligated Species **23**.* Rate values for **23**-catalyzed dehydrogenation run at 70 °C were determined using ^{11}B NMR as shown in the Supporting Information. In this reaction 7.7 mg of AB (0.25 mmol) was combined with (tube A) 20.7 mg of **23** (35 μmol, 14 mol %) and (tube B) 38.0 mg of **12** (35 μmol, 14 mol %). Data are shown in Table 4.

F. 1,10-Phenanthroline Poisoning Experiments. Fractional poisoning experiments employing separately 0.5, 0.1, and 0 mol equiv of 1,10-phenanthroline relative to [Ru_{atom}] were done under conditions otherwise identical with our standard conditions for ammonia−borane dehydrogenation by **12**.

1,10-Phenanthroline (2.2 mg, 12 μmol, 50 mol % versus [Ru_{atom}]) was added to a solution of 7.7 mg of ammonia−borane (0.25 mmol) and 13.6 mg of **12** (25 μmol, 5 mol % versus AB) in 0.6 mL of 2/1 diglyme/benzene-d_6. The rates for both the fast and slow catalysis cases at 70 °C were determined using ^{11}B NMR, as shown in the Supporting Information.

1,10-Phenanthroline (2.2 mg) was dissolved in 0.5 mL of diglyme to make a 1,10-phenanthroline stock solution. A portion of this solution (0.1 mL, 12 μmol, 10 mol % 1,10-phenanthroline versus [Ru_{atom}]) was added to a solution of 7.7 mg of ammonia−borane (0.25 mmol) and 13.6 mg of **12** (25 μmol, 5 mol % versus AB) in 0.5 mL of 2/1 diglyme/benzene-d_6. The rates for both the fast and slow catalysis cases at 70 °C were determined using ^{11}B NMR, as shown in the Supporting Information.

A further fractional poisoning regarding the role of 1,10-phenanthroline in the **26**-catalyzed dehydrogenation of ammonia−borane was also conducted. These data show little change in reactivity upon addition of the poison (see the Supporting Information).

III. Preparative and Spectroscopic Details for Adduct 23. The Ru−NH_3 adduct **23** was prepared by delivering ammonia gas to a benzene (5 mL) solution of **18** (50 mg, 0.046 mmol). The reaction mixture was stirred at room temperature for 15 min. A black precipitate was filtered out and successively washed with deionized water, acetone, benzene, and hexanes. The solid was then dried under vacuum to give a pale gray powder in 59% yield (30 mg).

^{1}H NMR (pyridine-d_5, 600 MHz): δ 8.05 (d, J_{HH} = 7.1 Hz, 4H, Ph), 7.47 (d, J_{HH} = 7.1 Hz, 4H, Ph), 7.18 (t, J_{HH} = 7.1 Hz, 4H, Ph), 7.13 (m, 6H, Ph), 7.07 (t, J_{HH} = 7.1 Hz, 4H, Ph), 4.25 (br. s, 3H, NH_3). ^{13}C{^{1}H} NMR (pyridine-d_5, 150 MHz): δ 202.5 (CO), 165.5 (C_1 of Cp), 134.9 (Ph), 133.4 (Ph), 133.2 (Ph), 131.3 (Ph), 128.5 (Ph), 128.4 (Ph), 128.3 (Ph), 126.9 (Ph), 104.3 ($C_{2,5}$ of Cp), 83.0 ($C_{3,4}$ of Cp). Data are consistent with a known compound.[23]

■ ASSOCIATED CONTENT

Ⓢ Supporting Information

Text and figures giving further experimental details and data. This material is available free of charge via the Internet at http://pubs.acs.org.

■ AUTHOR INFORMATION

Corresponding Author

*E-mail: travisw@usc.edu.

Notes

The authors declare no competing financial interest.

■ ACKNOWLEDGMENTS

We thank Richard Finke and Ercan Bayram (Colorado State) for insightful discussions. This work was sponsored by the National Science Foundation (CHE-1054910) and the Hydrocarbon Research Foundation. We are grateful to the National Science Foundation (DBI-0821671, CHE-0840366), the National Institutes of Health (1 S10 RR25432), and the University of Southern California for their sponsorship of NMR spectrometers at USC.

■ REFERENCES

(1) (a) Imarisio, G. *Int. J. Hydrogen Energy* **1981**, *6*, 153−158. (b) Zoulias, E.; Varkaraki, E.; Lymberopoulos, N.; Christodoulou, C. N.; Karagiorgis, G. N. *TCJST* **2004**, *4*, 41−71. (c) Liu, R.-S.; Zhang, L.; Sun, X.; Liu, H.; Zhang, J. Water Electrolysis for Hydrogen Generation, In *Electrochemical Technologies for Energy Storage and Conversion*; Millet, P., Ed., Wiley-VCH: Weinheim, Germany, 2011; Vol. *1*, p 2.

(2) United States Department of Energy, Hydrogen Fuel Cells and Infrastructure Technology Program. *Multi-Year Research Development and Demonstration Plan*, General Printing Office: Washington, DC, 2009; Section 3.3.

(3) Satyapal, S.; Petrovic, J.; Read, C.; Thomas, G.; Ordaz, G. *Catal. Today* **2007**, *120*, 246−256.

(4) For a review, see: (a) Staubitz, A.; Robertson, A. P. M.; Manners, I. *Chem. Rev.* **2010**, *110*, 4079−4124. For thermolysis of ammonia−borane see: (b) Baitalow, F.; Wolf, G.; Jaeicke-Rossler, K.; Leitner, G. *Thermochim. Acta* **2006**, *445*, 121−125. (c) Baitalow, F.; Baumann, J.; Wolf, G.; Jaenicke-Rossler, K.; Leitner, G. *Thermochim. Acta* **2002**, *391*, 159−168. (d) Wolf, G.; Baumann, J.; Baitalow, F.; Hoffmann, F. P. *Thermochim. Acta* **2000**, *343*, 19−25. (e) Wang, J. S.; Geanangel, R. A. *Inorg. Chim. Acta* **1988**, *148*, 185−190. (f) Bluhm, M. E.; Bradley, M. G.; Butterick, R., III; Kusari, U.; Sneddon, L. G. *J. Am. Chem. Soc.* **2006**, *128*, 7748−7749. (g) Rassat, S. D.; Aardahl, C. L.; Autrey, T.; Smith, R. S. *Energy Fuels* **2010**, *24*, 2596−2606. (h) Nylen, J.; Sato, T.; Soignard, E.; Yarger, J. L.; Stoyanov, E.; Haussermann, U. *J. Chem. Phys.* **2009**, *131*, 104506. (i) Heldebrant, D. J.; Karkamakar, A.; Hess, N. J.; Bowden, M.; Rassat, S.; Zheng, F.; Rappe, K.; Autrey, T. *Chem. Mater.* **2008**, *20*, 5332−5336. For hydrolysis, see: (j) Marder, T. B. *Angew. Chem., Int. Ed.* **2007**, *46*, 8116−8118. (k) Yan, J. M.; Zhang, X. B.; Akita, T.; Haruta, M.; Xu, Q. *J. Am. Chem. Soc.* **2010**, *132*, 5326−5327. (l) Jiang, H. L.; Umegaki, T.; Akita, T.; Zhang, X. B.; Haruta, M.; Xu, Q. *Chem. Eur. J.* **2010**, *16*, 3132−3137. (m) Ramachandran, P. V.; Gagare, P. D. *Inorg. Chem.* **2007**, *46*, 7810−7817.

(5) (a) Stephens, F. H.; Pons, V.; Baker, R. T. *Dalton Trans.* **2007**, 2613−2626. (b) Smythe, N. C.; Gordon, J. C. *Eur. J. Inorg. Chem.* **2010**, 509−521. (c) Hamilton, C. W.; Baker, R. T.; Staubitz, A.; Manners, I. *Chem. Soc. Rev.* **2009**, *38*, 279−293. (d) Sutton, A. D.; Burrell, A. K.; Dixon, D. A.; Gardner., E. B.; Gordon, J. C.; Nakagawa, T.; Ott, K. C.; Robinson, J. P.; Vasiliu, M. *Science* **2011**, *331*, 1426−1429.

(6) (a) Jaska, C. A.; Templ, K.; Lough, A. J.; Manners, I. *J. Am. Chem. Soc.* **2003**, *125*, 9424−9434. (b) Jaska, C. A.; Manners, I. *J. Am. Chem. Soc.* **2004**, *126*, 1334−1335. (c) Sgrestha, R. P.; Diyabalanage, H. V. K.; Semelsberger, T. A.; Ott, K. C.; Burrell, A. K. *Int. J. Hydrogen Energy* **2009**, *34*, 2616−2621. Regarding borane−Rh coordination, see: (d) Douglas, T. M.; Chaplin, A. B.; Weller, A. S. *J. Am. Chem. Soc.* **2008**, *130*, 14432−14433. (e) Alcaraz, G.; Sabo-Etienne, S. *Angew. Chem., Int. Ed.* **2010**, *49*, 7170−7179.

(7) Denny, M. C.; Pons, V.; Hebdon, T. J.; Heinekey, M.; Goldberg, K. I. *J. Am. Chem. Soc.* **2006**, *128*, 12048−12049.

(8) Blaquiere, N.; Diallo-Garcia, S.; Gorelsky, I.; Black, A.; Fagnou, K. *J. Am. Chem. Soc.* **2008**, *130*, 14034−14035. (f) Käβ, M.; Fridrich, A.; Drees, M.; Schneider, S. *Angew. Chem., Int. Ed.* **2009**, *48*, 905−907.

(9) Conley, B. L.; Williams, T. J. *Chem. Commun.* **2010**, *46*, 4815−4817.

(10) Conley, B. L.; Guess, D.; Williams, T. J. *J. Am. Chem. Soc.* **2011**, *133*, 14212−14215.
(11) Keaton, R. J.; Blacquiere, J. M.; Baker, R. T. *J. Am. Chem. Soc.* **2007**, *129*, 1844−1845.
(12) Kim, S.-K.; Han, W.-S.; Kim, T.-J.; Kim, T.-Y.; Nam, S. W.; Mitoraj, M.; Piecoś, Ł.; Michalak, A.; Hwang, S.-J.; Kang, S. O. *J. Am. Chem. Soc.* **2010**, *132*, 9954−9955.
(13) (a) Vance, J. R.; Robertson, A. P. M.; Lee, K.; Manners, I. *Chem. Eur. J.* **2011**, *17*, 4099−4103. (b) Baker, R. T.; Gordon, J. C.; Hamilton, C. W.; Henson, N. J.; Lin, P. H.; Maguire, S.; Murugesu, M.; Scott, B. L.; Smythe, N. C. *J. Am. Chem. Soc.* **2012**, *134*, 5598−5609.
(14) (a) Chapman, A. M.; Haddow, M. F.; Wass, D. F. *J. Am. Chem. Soc.* **2011**, *133*, 8826−8829.
(15) Conley, B. L.; Pennington-Boggio, M. K.; Boz, E.; Williams, T. J. *Chem. Rev.* **2010**, *110*, 2294−2312.
(16) (a) Wright, W. R. H.; Berkeley, E. R.; Alden, L. R.; Baker, R. T.; Sneddon, L. G. *Chem. Commun.* **2011**, *47*, 3177−3179. (b) Alcaraz, G.; Vendier, L.; Clot, E.; Sabo-Etienne, S. *Angew. Chem., Int. Ed.* **2010**, *49*, 918−920.
(17) Conley, B. L.; Williams, T. J. *J. Am. Chem. Soc.* **2010**, *132*, 1764−1765.
(18) (a) Casey, C. P.; Singer, S. W.; Powell, D. R.; Hayashi, R. K.; Kavana, M. *J. Am. Chem. Soc.* **2001**, *123*, 1090−1100. (b) Casey, C. P.; Beetner, S. E.; Johnson, J. B. *J. Am. Chem. Soc.* **2008**, *130*, 2285−2295. (c) Casey, C. P.; Johnson, J. B.; Singer, S. W.; Cui, Q. *J. Am. Chem. Soc.* **2005**, *127*, 3100−3109.
(19) Johnson, J. B.; Bäckvall, J.-E. *J. Org. Chem.* **2003**, *68*, 7681−7684.
(20) Thorson, M. K.; Klinkel, K. L.; Wang, J.; Williams, T. J. *Eur. J. Inorg. Chem.* **2009**, 295−302.
(21) Hu, M. G.; Van Paasschen, J. M.; Geanangel, R. A. *J. Inorg. Nucl. Chem.* **1997**, *39*, 1247−1250.
(22) Koren-Selfridge, L.; Query, I. P.; Hanson, J. A.; Isley, N. A.; Guzei, I. A.; Clark, T. B. *Organometallics* **2010**, *29*, 3896−3900.
(23) Hollmann, D.; Jiao, H.; Spannenberg, A.; Bähn, S.; Tillack, A.; Parton, R.; Altink, R.; Beller, M. *Organometallics* **2009**, *28*, 473−479.
(24) Stephens, F. H.; Pons, V.; Baker, R. T. *Dalton Trans.* **2007**, 2613−2626.
(25) Hagen, C. M.; Vieille-Petit, L.; Laurenczy, G.; Süss-Fink, G.; Finke, R. G. *Organometallics* **2005**, *24*, 1819−1831.
(26) (a) Widegren, J. A.; Finkie, R. G. *J. Mol. Catal.* **2003**, *198*, 317−341. (b) Kovács, G.; Nádasdi, L.; Joó, F.; Laurenczy, G. *C. R. Acad. Sci. Paris, Chim.* **2000**, *3*, 601.
(27) Bayram, E.; Linehan, J. C.; Fulton, J. L.; Roberts, J. A. S.; Szymczak, N. K.; Smurthwaite, T. D.; Özkar, S.; Balasubramanian, M.; Finke, R. G. *J. Am. Chem. Soc.* **2011**, *133*, 18889−18902.
(28) Wildeman, T.; Sneddon, L. G. *Inorg. Chem.* **1995**, *34*, 1002−1003.